

# Fabrication Process for Barium Titanate–Ferrite Functionally Graded Ceramics

S. Sarraute,<sup>a</sup> O. Toft Sørensen<sup>a\*</sup> and E. Rubæk Hansen<sup>b</sup>

<sup>a</sup>Risø National Laboratory, Materials Department, Roskilde, Denmark

<sup>b</sup>Ferroperm Components, Division of AMP Denmark, Helsingør, Denmark

(Received 14 July 1997; accepted 20 November 1997)

## Abstract

*The purpose of this work is to develop a fabrication process to produce barium titanate–ferrite functionally graded multilayer ceramics by dry pressing. Two materials were used; a dielectric powder based on BaTiO<sub>3</sub> and a magnetic Ni–Zn ferrite which were co-sintered. Two types of cracks were observed after sintering. A Scanning Electron Microscopy (SEM) examination of the sintered samples was performed in order to determine whether the cracks appear during the forming method or are due to thermal mismatching between the two materials. A crack free non symmetric configuration multilayer was obtained by sequentially stacking, pressing and sintering. © 1998 Elsevier Science Limited. All rights reserved*

*Le but de ce travail est de développer une méthode de fabrication pour fabriquer des céramiques multicouches fonctionnelles titanate de barium-ferrite par pressage à sec. Deux composés sont utilisés, une poudre diélectrique basée sur BaTiO<sub>3</sub> et un ferrite Ni–Zn qui sont frittés simultanément. Deux sortes de fissures sont observées après frittage. Une étude des échantillons frittés a été réalisée au microscope électronique à balayage (MEB) pour déterminer si les fissures apparaissent lors du pressage ou sont dues à la différence des coefficients de dilatation thermique des deux composés. Une multicouche sans fissures de configuration non symétrique a été obtenue par empilement séquentiel, pressage et frittage.*

## 1 Introduction

Functionally graded ceramics are a new class of materials in which it is possible to obtain a gradient of properties which cannot be obtained in any

monolithic ceramics. Several techniques are usually used to fabricate these materials such as tape casting,<sup>1,2</sup> sequentially slip casting<sup>3,4</sup> or self-propagating high temperature synthesis (SHS).<sup>5</sup>

The method described in this paper is very simple and less expensive than those methods currently used. The two materials used, a dielectric powder based on BaTiO<sub>3</sub> (commercial X7R) (DP) and a modified magnetic Ni–Zn ferrite [A or B: (Ni,Zn)-Fe<sub>2</sub>O<sub>4</sub>, A and B differs by a small amount of modifier] were dry pressed using different processes and sintered together at high temperature into one rigid component. The exact composition of the starting powders are proprietary. The main problem that arises is due to the thermal mismatch between the two materials. To avoid this during the sintering some mixed composition powders were prepared and characterised using several techniques. With these powders, some multilayers were sintered. The samples were then examined by SEM to determine the validity of the process and to obtain information on how to prevent thermal cracking. Two kinds of cracks were observed and were both eliminated producing crack free non-symmetric configuration multilayers.

## 2 Experimental

### 2.1 Preparation of the mixed composition powders

The mixed composition powders were prepared either by ball milling or by grinding in a mortar. For both methods, the pure powders used had a characteristic grain size and did not contain binder.

#### 2.1.1. Ball milling method

Two wt% of the binder Mobil CERQ (based on vax microemulsion) was added and the powders were ball milled in demineralized water for 4 h. The powders obtained were dried at 100°C in a drying oven. The mixed composition powders were then

\*To whom correspondence should be addressed.

ready to be used for the preparation of the multilayers or for characterisation.

### 2.1.2. Grinding

The first step was to ball mill separately the dielectric powder (DP) and the ferrite using the conditions described above. Then, the two powders (DP and ferrite A or B) were ground together in a mortar.

## 2.2 Characterisation

### 2.2.1. Mixed composition powders

The first step of characterisation of the mixed composition powders was to obtain their X-ray diffraction patterns. In this way, the composition of the ceramics is controlled.

### 2.2.2. Mixed composition ceramics

X-ray diffraction patterns were obtained for each ceramics in order to check the composition and to detect whether a chemical reaction had taken place during the sintering. Some physical properties of the ceramics were also measured: the density using Archimedes method in water, the grain size using SEM, thermal expansion coefficient using dilatometry and the permittivity using a capacitance bridge.

## 2.3 Fabrication of multilayers

The multilayers were fabricated by dry pressing. The following multilayers used were, in a first step:

1. ferrite A and DP with MPB (mixed powder composed of 50% of ferrite A and 50% of DP) as an interlayer: ML2 (A-MPB-DP-MPB-A);
2. ferrite B and DP with MPBB (mixed powder composed of 50% of ferrite B and 50% of DP) as an interlayer: ML4 (B-MPBB-DP-MPBB-B).

In a second step, two other multilayers were prepared:

1. A and DP with MPB and the mixed powder 20/80 (MPB1/4) as interlayers: ML21;
2. B and DP with MPBB and the mixed powder 20/80 (MPBB1/4) as interlayers: ML22.

ML21 and ML22 are also symmetric.

The multilayers were fabricated in two different shapes (pellet and bar) using the following four processes:

1. each layer was pressed separately and sintered under a load;
2. each layer was pressed separately and then, pressed together;

3. the first layer was pressed for 15 s, then the second layer was added in the same die as the first followed by pressing, until all the layers were pressed. For the last layer, the same pressure was applied for 1 min;
4. the first layer was manually compressed, then the second layer was added in the same die as the first, until all the layers were manually compressed and once the last layer was added in the same die, the structure was pressed for 1 min.

The pressure applied for the pellets was 127 MPa and 55 MPa for the bars. The sintering conditions used were the same for all multilayers which were sintered at 1120°C for 3 h.

## 2.4 Characterisation of multilayers

In order to obtain information on thermal cracking, SEM was performed with a low vacuum microscope (JSM-5310LV) where the samples do not need to be coated.

## 3 Results and Discussion

### 3.1 X-ray diffraction

In all the X-ray diffraction patterns of the mixed composition powders, the characteristic peaks of the two known phases of both powders introduced in the mixture were observed. These correspond to the spinel structure for the ferrite and to the perovskite structure for the dielectric. For the sintered ceramics, however, some additional peaks were observed. Comparing the diffraction pattern of these ceramics to the patterns in the JCPDS files, this extra phase was found to be a barium iron oxide. The additive of the ferrite are used to decrease the sintering temperature by creating a liquid phase at low temperature. This is probably why the Ni-Zn ferrite react with the barium titanate creating this phase. The quantity of this new phase is somewhat dependent on the ceramic observed. Fig. 1(a) and (b) represent the X-ray diffraction patterns of MPB powder and ceramic respectively. Also, Fig. 2(a) and (b) represent the X-ray diffraction patterns of MPBB before and after sintering, respectively. According to these patterns, this phase seems to be present in a large quantity in MPB but it is less important in MPBB. This is attributed to the fact that the amount of additive in ferrite B is less important than in ferrite A. The most important is that the fabrication of the multilayers is not affected by this reaction between the two materials.

### 3.2 Physical properties

Some of the characteristics of the obtained ceramics such as the permittivity  $\epsilon'_r$  at room temperature at

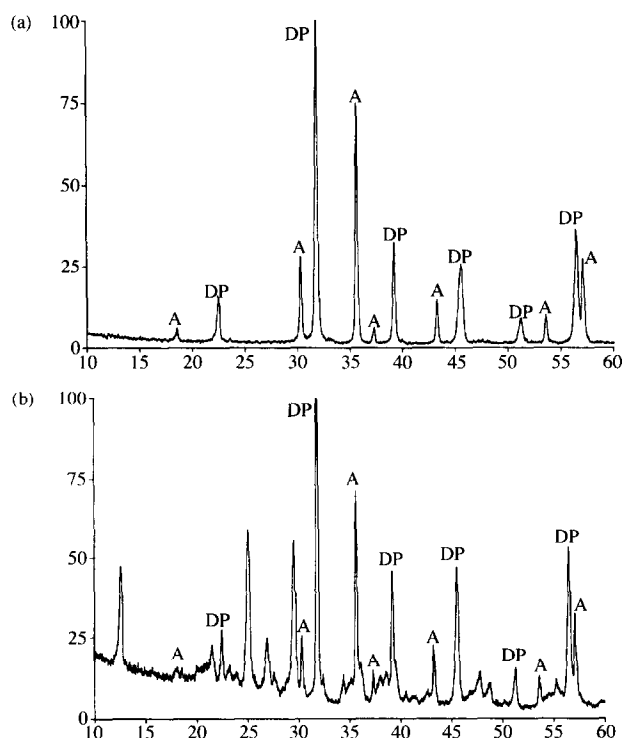


Fig. 1. X-ray diffraction patterns of (a) MPB powder and (b) ceramic.

1 kHz and 1 MHz, the density  $d$ , the grain size  $\phi$  and the thermal expansion coefficient  $\alpha$  are compared in Table 1 for the A-DP mixed composition and Table 2 for the B-DP one. The addition of ferrite, either A or B, leads to an important decrease of the permittivity values corresponding to an exponential behaviour between 20 to 90% or 20 to 80%, respectively. This exponential variation

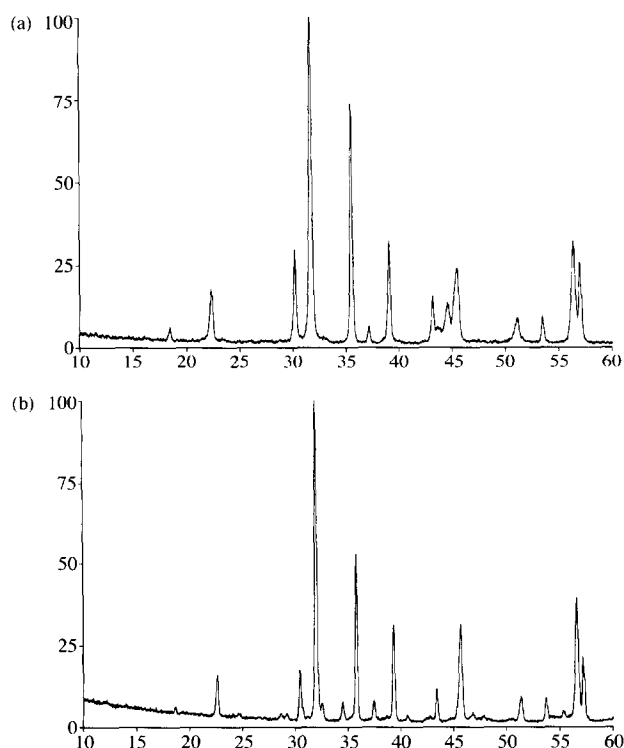


Fig. 2. X-ray diffraction patterns of (a) MPBB powder and (b) ceramic.

Table 1. Characteristics of the ceramics—A-DP mixed composition

wt% of DP in A	$\epsilon'_r$ (1 kHz)	$\epsilon'_r$ (1 MHz)	$d$ ( $g\ cm^{-3}$ )	$\phi$ (mm)	$\alpha\ 10^6$ ( $C^{-1}$ )
0	—	—	5.06 <sup>a</sup>	1.3 <sup>a</sup>	10.55 <sup>a</sup> (2)
20	46	33	5.31	1.3	10.0
	25 <sup>a</sup>	24 <sup>a</sup>	5.34 <sup>a</sup>	1.0 <sup>a</sup>	10.5 <sup>a</sup>
40	111	100	5.42 (4)	1.3	11.7
	66 <sup>a</sup>	61 <sup>a</sup>	5.53 <sup>a</sup>	1.1 <sup>a</sup>	11.2 <sup>a</sup>
50	82	76	5.48 (2)	1.3	10.9
	91 <sup>a</sup>	86 <sup>a</sup>	5.66 <sup>a</sup>	1.2 <sup>a</sup>	11.45 <sup>a</sup> (2)
60	156	144	5.36 (4)	1.3	11.9
	144 <sup>a</sup>	136 <sup>a</sup>	5.67 <sup>a</sup>	1.0 <sup>a</sup>	11.8 <sup>a</sup>
80	764	560	5.54	1.4	—
	301 <sup>a</sup>	283 <sup>a</sup>	5.84 <sup>a</sup>	1.1 <sup>a</sup>	12.5 <sup>a</sup>
100	1680 <sup>a</sup>	—	5.85 <sup>a</sup> (7)	1.2 <sup>a</sup>	14.15 <sup>a</sup>

<sup>a</sup>Ball-milling method.

The values in brackets represent the number of samples measured.

correspond to the mixing rules for a diphasic dielectric with a continuously connected phase.<sup>6</sup> The composition had no influence on the grain size. The thermal expansion coefficient and the density vary linearly with the composition for both ferrite A or B in the range composition from 20 to 80%. With the ball-milling method, the ceramics have:

1. higher density;
2. lower open porosity;
3. lower grain size;
4. homogeneous distribution between ferrite and dielectric grains (Figs 3 and 4).

The variation of the physical properties with the mass fraction is always linear between 20 to 80%. This can be also explained by percolation theory.<sup>7</sup>

### 3.3 Scanning electron microscopy (SEM) observations of sintered multilayers

The following observations were made on the samples prepared by the four processes: Process 1: ML4 was well bonded after sintering both with

Table 2. Characteristics of the ceramics—B-DP mixed composition

wt% of DP in B	$\epsilon'_r$ (1 kHz)	$\epsilon'_r$ (1 MHz)	$d$ ( $g\ cm^{-3}$ )	$\phi$ (mm)	$\alpha\ 10^6$ ( $C^{-1}$ )
0	—	—	4.98 <sup>a</sup>	1.2 <sup>a</sup>	10.1 <sup>a</sup>
20	34	22	5.14	1.4	9.1
	24 <sup>a</sup>	22 <sup>a</sup>	5.35 <sup>a</sup>	1.0 <sup>a</sup>	10.7 <sup>a</sup>
40	62	56	5.36 (4)	1.2	9.1
	59 <sup>a</sup>	55 <sup>a</sup>	5.47 <sup>a</sup>	1.1 <sup>a</sup>	11.1 <sup>a</sup>
50	168	149	5.23 (2)	1.4	10.3
	126 <sup>a</sup>	119 <sup>a</sup>	5.66 <sup>a</sup>	1.3 <sup>a</sup>	11.45 <sup>a</sup>
60	102	94	5.61	1.2	8.4
	133 <sup>a</sup>	125 <sup>a</sup>	5.71 <sup>a</sup>	1.1 <sup>a</sup>	11.8 <sup>a</sup>
80	303	252	5.40	1.5	10.7
	336 <sup>a</sup>	313 <sup>a</sup>	5.83 <sup>a</sup>	1.1 <sup>a</sup>	12.7 <sup>a</sup>
100	1680 <sup>a</sup>	—	5.85 <sup>a</sup> (7)	1.2 <sup>a</sup>	14.15 <sup>a</sup> (2)

<sup>a</sup>Ball-milling method.

The values in brackets represent the number of samples measured.

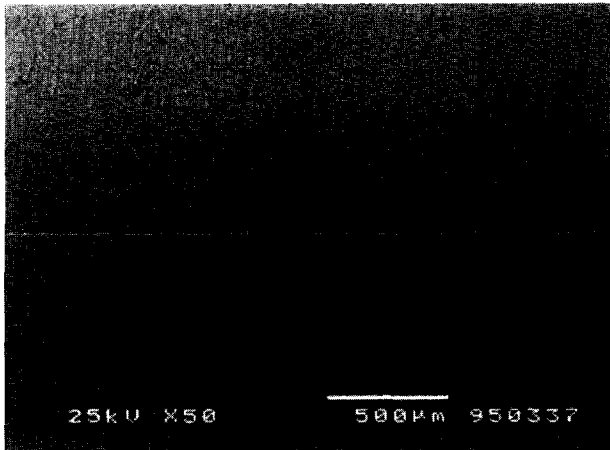


Fig. 3. MPBB made by ball-milling.

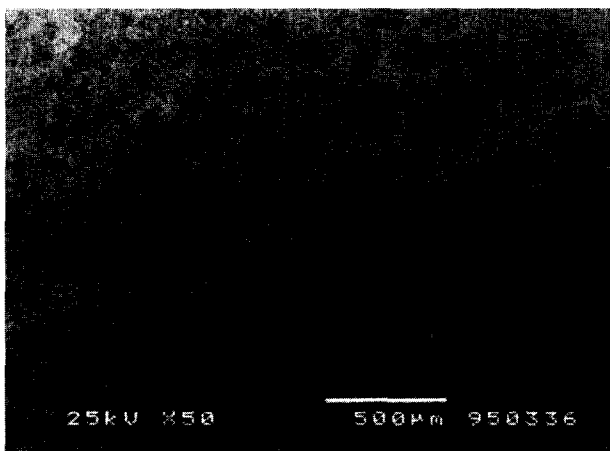


Fig. 4. MPBB made by grinding.

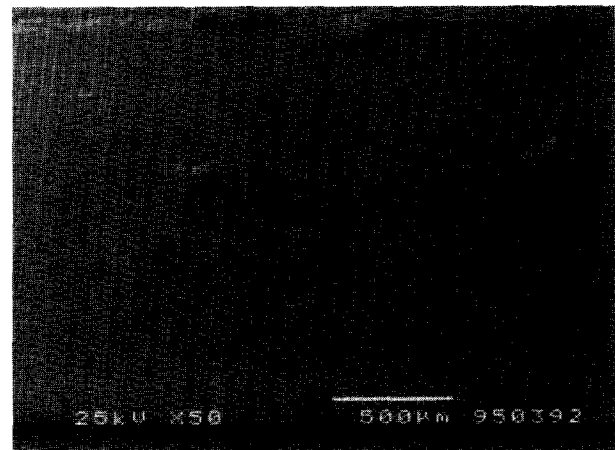


Fig. 5. ML4 made with process 1 (bar shape): cracks in DP layer.

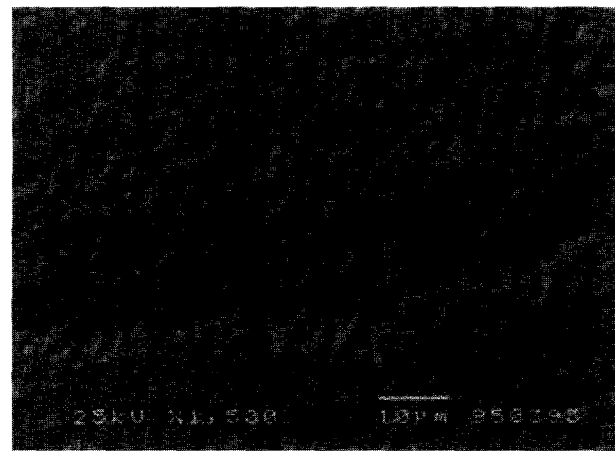


Fig. 6. ML4 made with process 2 (pellet shape): interface MPBB-DP.

pellet and bar shapes. Fig. 5 shows many cracks in the dielectric layer of ML4. These cracks extended through the dielectric layer and stopped at the interface with the mixed composition layer. For this sample, no other cracks were observed. For this process, ML2 was not bonded.

Process 2: The two multilayers (ML2 and ML4) were well bonded after sintering. Fig. 6 shows a crack extending through the interface between the dielectric and the mixed composition layers of ML4. At this interface, special grain shapes were observed. This crack stopped at the interface between the mixed composition and the ferrite layers. EDX (Electron Diffraction X-ray) analysis was performed on this multilayer with a high vacuum microscope (JSM-820) to determine the composition of the special grain shapes. There was no detectable diffusion from one layer to another but the presence of iron was detected in the dielectric layer near the interface with the mixed composition layer. This confirms the appearance of a barium iron oxide observed by X-ray diffraction. ML2, produced with this process, had cracks in all the layers. Cracks were also observed along the dielectric and mixed composition layers interface.

Process 3: The two multilayers, with the pellet shape, were also well bonded, whereas it only worked for ML2 with the bar shape. For ML4, a delamination near the interface between the dielectric and the mixed composition layers was observed (Fig. 7). Cracks were observed in all the layers of ML4 and especially at the dielectric and the mixed composition layer interface. Cracks were observed at the interface and also at the ferrite and mixed composition layer interface and in the dielectric layer. As for ML4, cracks were observed in all the layers of ML2 and also at the interface. The crack between the ferrite and the mixed composition layers extended as a straight line.

With the three processes used, cracks were observed in all multilayers. Sintering experiment was performed to discover at which step of the multilayer fabrication the cracks appeared. In this experiment, ML4 samples were heated in several steps to the sintering temperature and then examined for cracks after cooling. Cracks were already observed at the green stage and were situated near the interface; their directions were always parallel to the interface. The pressing processes thus induce cracks in the multilayers. On the other hand,

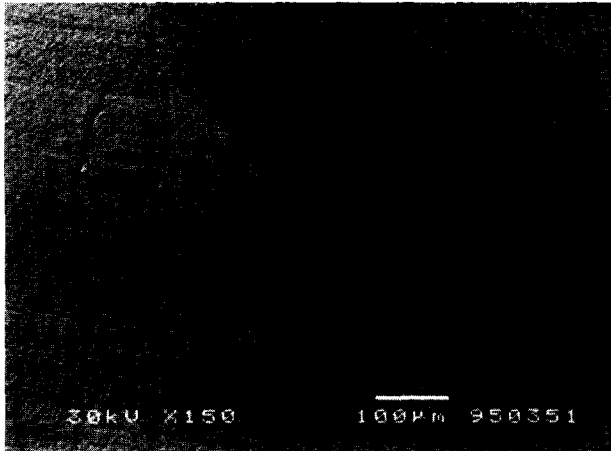


Fig. 7. ML4 made with process 3 (bar shape): start of the delamination in MPBB layer near the interface with DP.

cracks perpendicular to the interface appear only at the sintering temperature. Cracks formed during pressing are thus always present in these samples. The final sintered sample hence contain both types of cracks. (Figs 8 and 9).

Process 4: No cracks were observed at the green stage for ML4, but after sintering, cracks appeared in the dielectric and the mixed composition layers. These cracks were thinner and fewer compared to

the previous one observed in the other processes (Figs 10 and 11). The same process was used for ML2 and cracks extended through the dielectric layer, through the mixed composition layer and then, stopped at the ferrite interface. The crack size decreased as it extended toward the ferrite layer. Small cracks were also observed at the interface between the dielectric and the mixed layers but not at the other interfaces. These cracks were only due to the thermal mismatching between the layers. To prevent these cracks, introduction of more mixed composition layers is therefore necessary.

Using process 4, ML22 and ML21 were produced. Few cracks were observed in ML22 and these extended through all the layers except the ferrite layer as a straight line. Looking at the cross section of this sample, the crack size decreased from the dielectric layer to the mixed composition layers to stop at the ferrite interface (Fig. 12). ML21 was well bonded and cracks were observed in all the layers. For the bar shape, many cracks were observed inside the dielectric layer and others extended through all the layers. For the pellet shape, few cracks were observed and these extended through all layers except the ferrite. Crack-free

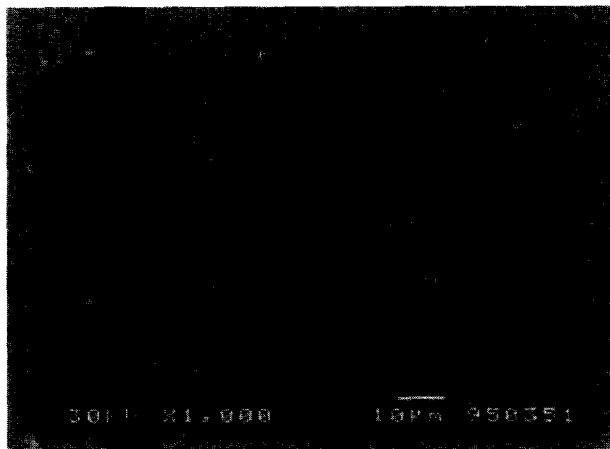


Fig. 8. ML4 at the green stage: interface DP-MPBB.

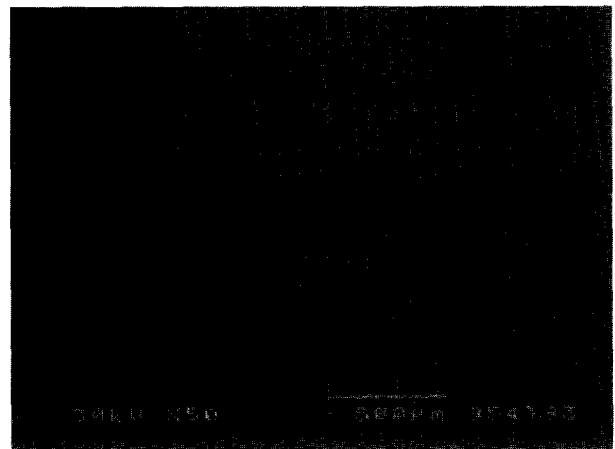


Fig. 10. ML4 made with process 4 (pellet shape): green stage.

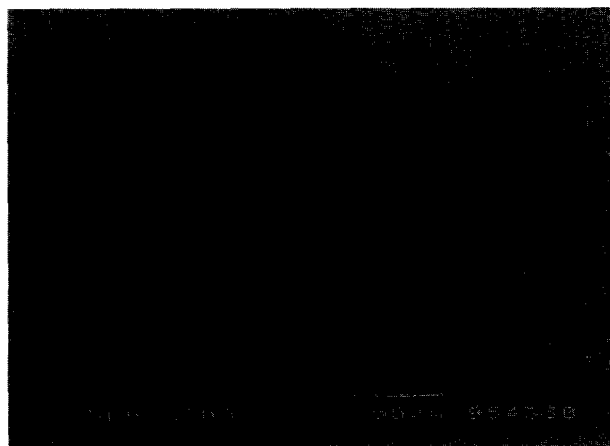


Fig. 9. ML4 sintered: interface MPBB-DP.

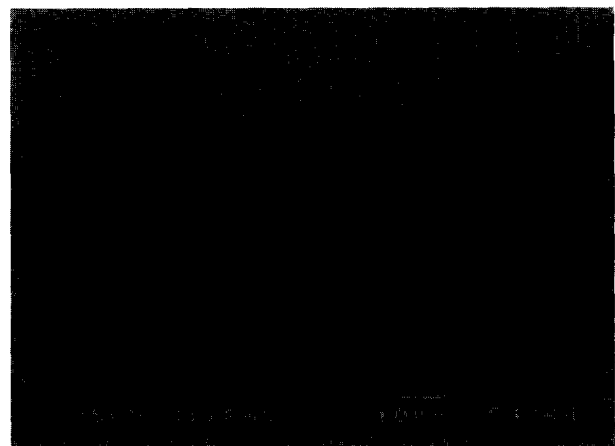


Fig. 11. ML4 made with process 4 (pellet shape): interface DP-MPBB.

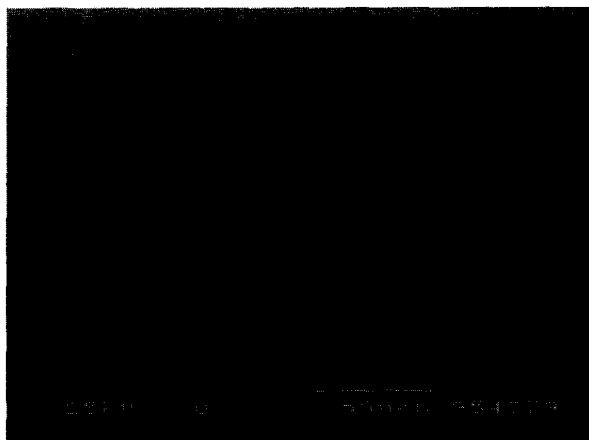


Fig. 12. ML22 process 4 (pellet shape): cross-section of the multilayer.

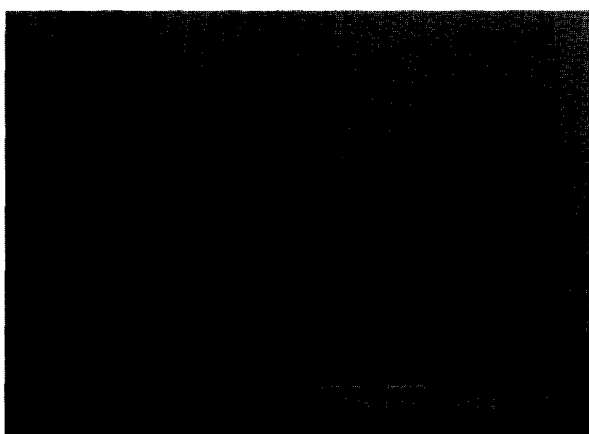


Fig. 13. ML22 non-symmetric crack-free ceramic.

ceramics were made with the non symmetric system of ML21 and ML22 using process 4 (Fig. 13).

Furthermore, a theoretical model of the multilayer mechanical behaviour was developed to explain the experimental results and especially the delamination of the samples.<sup>8</sup> This model calculates the energy release rate at each interface of the multilayer taking into account the thermal expansion coefficient, the elastic properties and the thickness of each layer. If this energy release rate is higher than the fracture energy then a crack will propagate all through the sample. Therefore, to obtain crack free ceramics, the energy release rate must be reduced. The calculation shows three important parameters: the number of layers, the total thickness and the thickness of the interlayers compared to the total thickness. In accordance with this modelling, crack-free non-symmetric

samples were fabricated by reducing the total thickness of the ceramic multilayer.

#### 4 Conclusions

Ball-milling is the best way to prepare the mixed composition powders. The dielectric powder and ferrite A or B react together during the sintering creating a barium iron oxide. This reaction depends somewhat on the ratio between the two materials of the mixed powder. This phase seems also to have no influence on the bonding of the multilayers.

Two kinds of cracks were detected: cracks induced by the forming method used and those induced by thermal mismatching between the layers. Both of these could be eliminated: cracks due to the forming method by using a sequential stacking and pressing process (process 4) and the cracks due to thermal mismatching by using two different mixed composition layers as interlayers. This process leads to crack free ceramics and can also probably be used to co-sinter other materials.

#### References

1. Nieto, E., Fernandez, J. F., Moure, C. and Duran, P., Multilayer piezoelectric devices based on PZT. *J. Mater. Sci.: Materials in Electronics*, 1996, **7**, 55–60.
2. Wu, C. C. M., Kahn, M. and Moy, W., Piezoelectric ceramics with functional gradients: A new application in material design. *J. Am. Cer. Soc.*, 1996, **79**, 809–812.
3. Moya, J. S., Sanchez-Herencia, A. J., Requena, J. and Moreno, R., Functionally gradient ceramics by sequential slip casting. *Mater. Lett.*, 1992, **14**, 333–335.
4. Pena, P., Bartolome, J., Requena, J. and Moya, J. S., Mullite-alumina functionally gradient ceramics. *J. de Phys. IV*, 1993, **3**, 1261–1266.
5. Miyamoto, Y., Li, Z. and Tanihata, T., Recycling processes of Si waste to advanced ceramics using SHS reaction. *Ann. Chim. Fr.*, 1995, **20**, 197–203.
6. Payne, D. A. and Cross, L. E., Microstructure—property relations for dielectric ceramics: I. Mixing of isotropic homogeneous linear dielectrics, In *Ceramics Microstructures*, ed. R. M., Tullath and J. A. Pask. Westview Press, Boulder, CO, 1976, pp. 584–597.
7. Sarraute, S., Sørensen, O. T., Hansen, E. R. and Sørensen, B. F., Microstructure dependent thermophysical properties of Ni–Zn ferrite/BaTiO<sub>3</sub> functionally graded ceramics (to be submitted).
8. Sørensen, B. F., Sarraute, S., Jørgensen, O. and Horsewell, A., Thermally induced delamination of multilayers. *Acta. Met.*, (submitted).